Numerical simulation of a 3-D laminar wing in transonic regime

D. Szubert[1,2], I. Asproulias[1], N. Simiriotis[1], Y. Hoarau[3], M. Braza[1]

Abstract
The present paper details the simulations carried out for the 3D-V2C wing configuration designed by Dassault Aviation in the context of the TFAST - Transition location effect on shock boundary layer interaction - European programme. The results concern the constant section wing and the swept one. In the second case, the transition location is imposed by numerical tripping of the eddy-viscosity to examine the impact of its location on the buffet's onset. The computations have been carried out by using URANS, OES and hybrid approaches. The results analyse the transonic buffet dynamics by means of spectral and POD analysis in case of the constant section wing. They also examine onset of unsteadiness at 5° and 7° of incidence for the swept wing. Because of the chord's length variation, there are sections where the local Reynolds number is subcritical or supercritical regarding the buffet instability.

1 Introduction

The present study has been analysed within the TFAST (Transition location effects on shock boundary layer interaction) EU program to study the buffet dynamics in case of a constant section supercritical wing, as well as in case of a swept wing, by means of statistical and hybrid turbulence modelling. One of the main objectives of this research is to provide optimal laminarity in the boundary layer upstream of the shockwave/ boundary-layer interaction (SWBLI) to reduce the skin friction comparing to the fully turbulent case and therefore reduce drag, in the context of greening aircraft transport (a major objective of the Horizon 2020 European programme). Due to increased aerodynamic loads and aero-engine components nowadays, supersonic flow velocities are more frequent, generating shock waves that interact with boundary layers. Laminar shockwave/ boundary-layer interaction can rapidly cause flow separation, which is highly detrimental to aircraft performance and poses a threat to safety. This situation can be improved

[1] D. Szubert, I. Asproulias, N. Simiriotis, M. Braza : Institut de Mécanique des Fluides de Toulouse, UMR CNRS 5502, email: Marianna.Braza@imft.fr
[2] D. Szubert, DGA Th, Techniques Hydrodynamiques, damien.szubert@intradef.gouv.fr
[3] Y. Hoarau: ICUBE, UMR CNRS 7357, Strasbourg University, email: hoarau@unistra.fr

by imposing the laminar-turbulent transition upstream of the interaction, but this should be carefully done in order to keep the aerodynamic efficiency high (lift/drag ratio). In the context of the European research program TFAST, several ways of controlling the position of the transition are carried out. To this end, a supercritical laminar wing, the so called V2C, has been designed by Dassault Aviation. This profile allows the boundary layer to remain laminar up to the shock foot, even in the environment of transonic wind tunnels of the laboratories involved in the project, and up to the angle of attack of 7.0°. Regarding the related literature, the transonic buffet has been studied experimentally in detail since the 70s on circular-arc aerofoils (McDevitt *et al.* (1976), Seegmiller *et al.* (1974)) and most recently on supercritical aerofoils (Jacquin *et al.* (2009)). In this latest study, a fixed transition tripping was applied at 7% of the chord. The physics governing the transonic buffet is complex and several theories have been proposed, like the effect of the feedback mechanism of waves propagating from the trailing edge, or the onset of a global instability (Jaquin *et al.* (2009), Lee (1990), Szubert *et al.* (2015)). Comparison of numerical results by Deck (2005), Grossi *et al.* (2014) and Szubert *et al.* (2015) with the experimental results by Jacquin *et al.* (2005), concerning the transonic buffet around supercritical wings with fixed transition showed the predictive capability of recent CFD methods and a physical analysis of the interaction between buffet and trailing edge instabilities. The SWBLI (Shock Wave Boundary Layer Interaction) involving transonic buffet and laminar wing design currently highly interests the aeronautical industries (see for instance Cleansky European project, (2013-2016), "Advanced, high aspect ratio transonic laminar wing").

For the swept wing, a specific transition location has been selected, based on previous studies of us in this European programme, in order to capture the effects on the shock-boundary layer interaction. The present paper details the simulations carried out for the 3D-V2C swept wing configuration designed by Dassault Aviation in the context of the TFAST. The transition location is imposed by numerical tripping of the eddy-viscosity. Based on previous detailed studies, an optimal transition position at 55% of the chord has been investigated. In the present paper, the ability of statistical and hybrid turbulence modelling for capturing the flow physics arising with the buffet phenomenon will be investigated.

2 Test-case description, numerical parameters and turbulence modelling

The V2C wing designed by Dassault Aviation and used as a principal test-case of the TFAST European program. A first set of computations have been carried out for the 2D wing of constant section in the spanwise directions. The flow parameters for this part of the study are: a 0.25 m-chord length profile at freestream

Mach numbers of 0.70, yielding chord-based Reynolds number of approximately 3.245×10^6 respectively. The flow separated between $\alpha = 6°$ and 7°. The simulations have been carried out with the Navier–Stokes Multi-Block (NSMB) solver (Vos *et al.* 1998). The NSMB solver is the fruit of a European consortium that included Airbus from the beginning of 90s, as well as main European aeronautics research institutes like KTH, EPFL, IMFT, ICUBE, CERFACS, Karlsruhe Institute of Technology, ETH-Swiss Federal Institute of Technology in Zurich, among others. This consortium is coordinated by CFS Engineering in Lausanne, Switzerland. NSMB solves the compressible Navier–Stokes equations using a finite volume formulation on multi-block structured grids. For the present study, the third-order of accuracy Roe (1981) upwind scheme associated with the MUSCL flux limiter scheme of van Leer (1979) have been used. For the diffusion terms, second-order central differencing has been used. The temporal discretization has been done by means of dual-time stepping and of second order accuracy. A physical time step of 5 μs has been adopted for 2D simulations and of 10^{-7} s for the 3D simulations regarding the constant-section wing. The 2D grid's section has a C–H topology and is of size 163,584 cells. The downstream distance of the computational domain is located at a mean distance of 80 chords from the obstacle. A grid refinement study had been carried out prior to the present article, in the context of the PhD theses of F. Grossi and D. Szubert (IMFT). Concerning the swept V2C wing, the grid is of 9M finite-volume cells providing $y+$ values less than 0.03. The Mach number is 0.745 and the Reynolds number per meter is 4,47 x 10^6. The time-step is 10^{-5}s. The grids are presented in Figures 1 and 2.

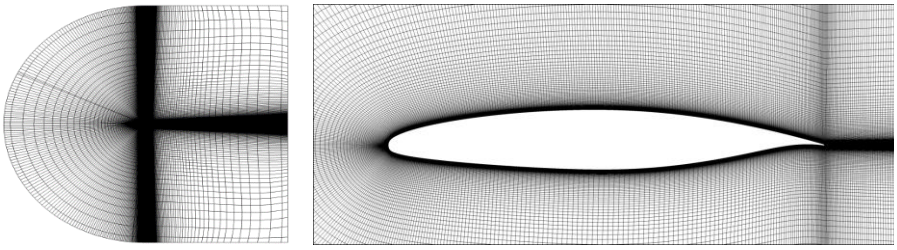

Fig.1 Constant section V2C wing: grid and zoom around the section

Boundary and initial conditions

On the solid wall, impermeability and no-slip conditions are employed. Concerning the far field boundary conditions, they are the characteristic variables extrapolated in time. Regarding the upstream free stream conditions, the total pressure (P0 = 10^5 Pa) and total temperature (T0 = 290 K), as well as the upstream Reynolds number of 3.245 million and Mach number of 0.70. The upstream turbulence intensity is Tu = 0.08%. Concerning the swept wing, the static pressure (free stream) is 17900 Pa, the total pressure 25900 Pa and the Temperature 241K. The inlet turbulence intensity Tu is 0.1% in this case. The initial conditions for both cases are those of a steady-state generated field.

Turbulence modelling
In the context of URANS and hybrid turbulence modelling, the following models have been used respectively: the two-equation k − ω SST model of Menter (1994) as well as the OES-k − ε (Braza *et al*. (2006), Bourguet *et al*. (2008)) and the DES-k − ω SST models (Spalart *et al*. (2006)) have been used with turbulence sustaining ambient terms (Spalart & Rumsey (2007)) to prevent the free decay of the transported turbulence variables.

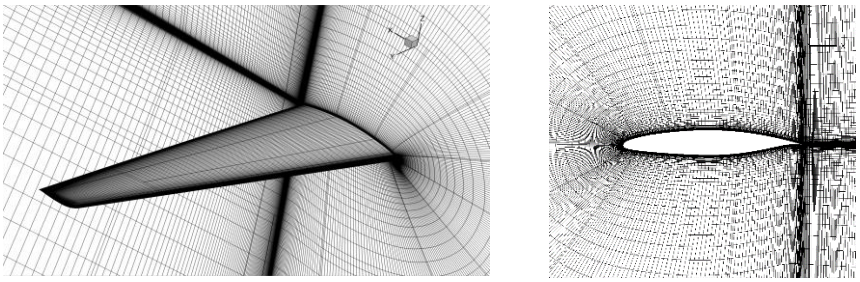

Fig. 2 Grid for the swept V2C wing: overview and zoom around a wing's section

3 Results

In the following, the results around the constant section 3D wing are presented, followed by those of the swept wing.

3.1 The constant-section V2C wing

In Figure 3, the buffet map is shown concerning the constant wing section case. The simulations carried out at 7° of incidence and free-stream Mach number correspond to buffet conditions. Indeed, in Figure 4, the buffet phenomenon is clearly illustrated, as well as its interaction with the shear layer and von Kármán eddies. Figure 5 shows the lift coefficient versus time, according to different turbulence models. The DDES-SST model provides a strong suction and creates a 'picky' behaviour of the lift coefficient oscillations. Table 1 shows the comparison of the mean values with experimental data measured by the Institute of Aviation (IoA) - TFAST co-partner. The strong suction effect of the DDES is seen on these values, where the OES modelling provides a good agreement. Figure 6 shows the lift coefficient spectra where the DDES-SST displays a quite spread spectrum bump around the buffet frequency. The OES approach provides a more pronounced spectral bump.

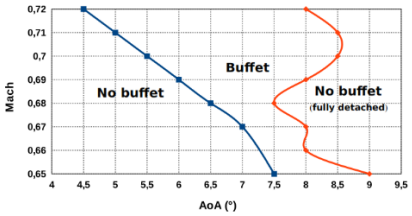

Fig.3 Buffet map

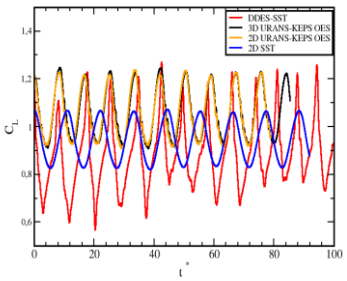

Fig.5 Lift coefficient oscillations for different turbulence models used

The dimensionless buffet frequency (Strouhal number) is of order 0.1, slightly varying from one model to the other (see the exact values displayed in the figure). Figure 7 shows iso-contours of the velocity vector divergence according to the DDES-SST and OES modelling.

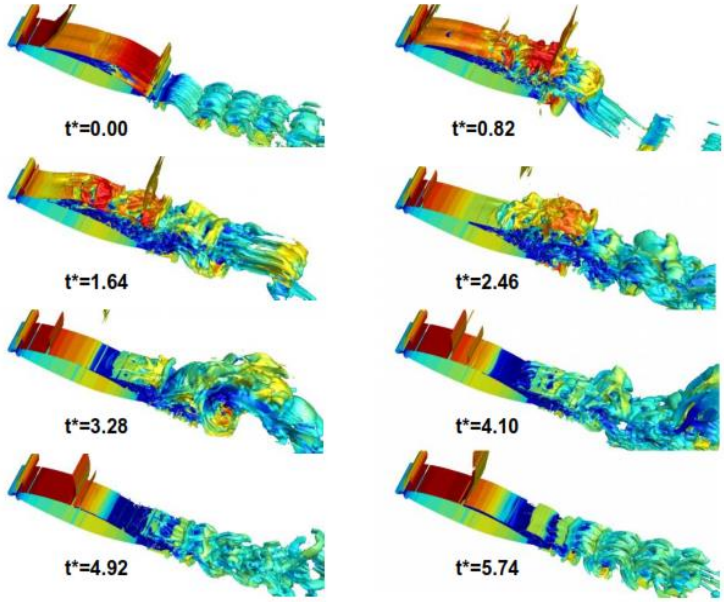

Fig.4 Instantaneous Q-criterion iso-surfaces for $Q(c/U)^2 = 75$. DDES-SST model

	EXPT	3D OES	2D OES	2D SST	DDES-SST
CL_avg	1.063	1.062	1.058	0.942	0.875
CD_avg	0.0815	0.0820	0.0811	0.0616	0.0902

Table 1. Constant section V2C wing: grid and zoom around the section

It is recalled the OES approach has also a hybrid character regarding the coherent /non-coherent distinction of the turbulence structures to be resolved/modeled and is classed in-between URANS and LES approaches, needing more economic grids than the LES one.
In order to analyze the buffet mode interaction with the shear layer dynamics and the near wake structures, 3D Proper Orthogonal Decomposition (POD), Berkooz *et al*. (1993) have been carried out in case of the DDES. Figure 8 shows the energy distribution of the POD modes which displays quite significant values up to the first decade of modes.

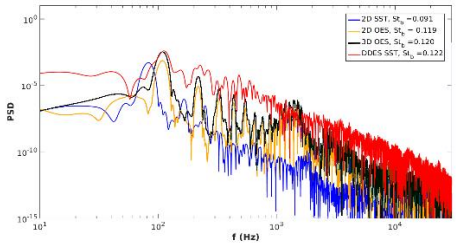

Fig.6 Spectra of the vertical velocity component

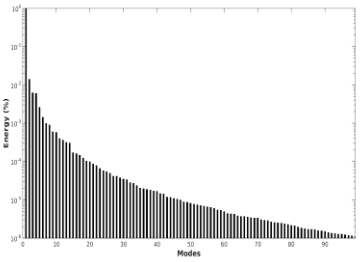

Fig.8 Energy distribution of the POD modes

The higher-order modes are also quite useful to be used for a stochastic forcing of the transport equations, able to constrict and thin the shear layers, by considerably reducing the eddy viscosity and improving the forces evaluation, as studied by Szubert *et al*. (2015). Figure 9 shows the spatial view of the low, intermediate and higher-order modes. In this figure, *w* designates the vertical velocity component, where *v* is the spanwise one. Mode 2 is clearly related to the buffet and the shock amplitude formation. Figure 10 shows the spectrum of the second-mode temporal coefficient which displays the spectral bump around the buffet frequency. It will be remembered that the fact of bump formation and not of a sharp peak indicates that the buffet in the present case is strongly affected by chaotic turbulence motion, enhanced by the strong suction. Figure 9 shows the spatial view of the 10^{th} mode, associated to the shear-layer dynamics. This is shown on the temporal coefficient spectrum of this mode (Fig.10) where the buffet bump has been attenuated on the profit of the shear layer frequency, near 3 x 10^3 Hz. The 30^{th} and 65^{th} spatial modes are enriched from the shear layer dynamics (Fig. 9). Concerning the spanwise velocity related to 3D effects, the 10^{th} and 30^{th} POD modes illustrate a chaotic formation of a multitude of spanwise wavelengths (Fig. 9).

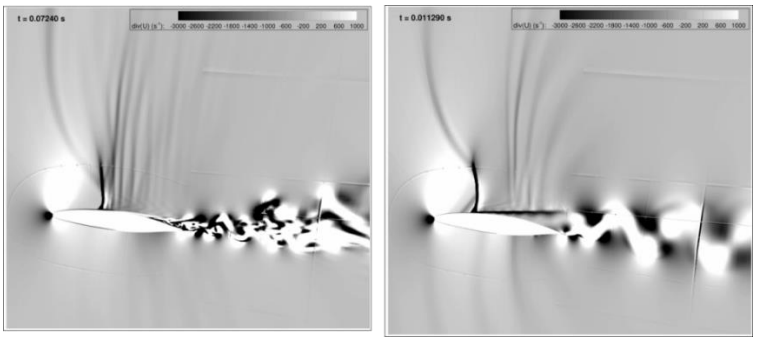

Fig.7 Instantaneous divergence of the velocity vector illustrating by numerical "Schlieren" visualization the shock wave, the Kutta waves, the SWBLI structure, the shear layer and von Kármán eddies. Left: DDES-SST, right: OES

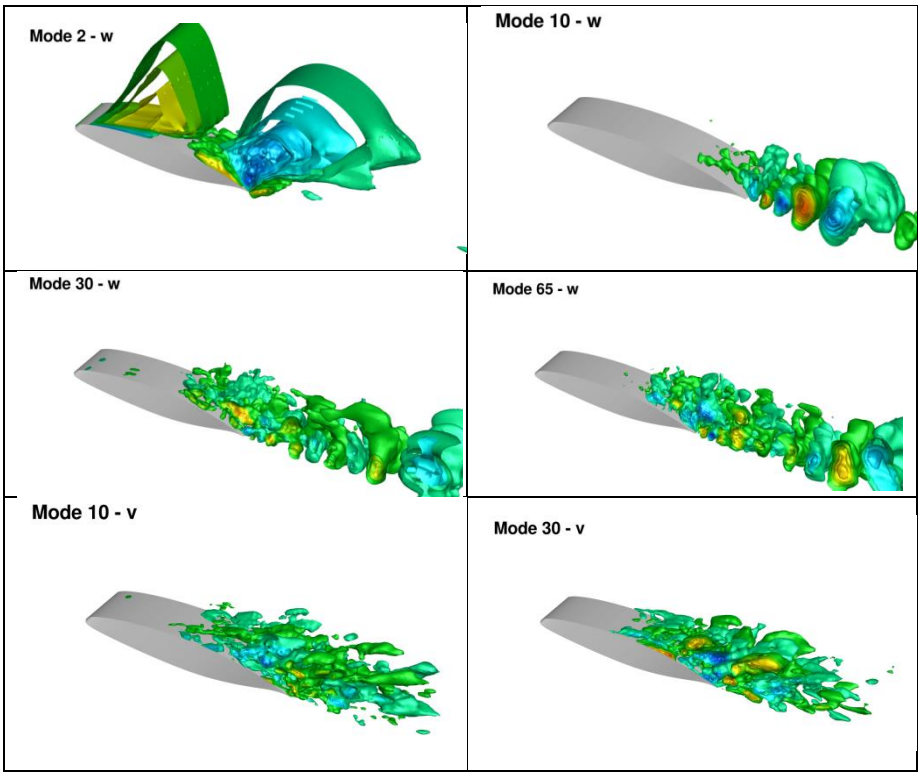

Fig.9 Spatial view of the POD modes: here *w* is the vertical velocity and *v* is the spanwise one.

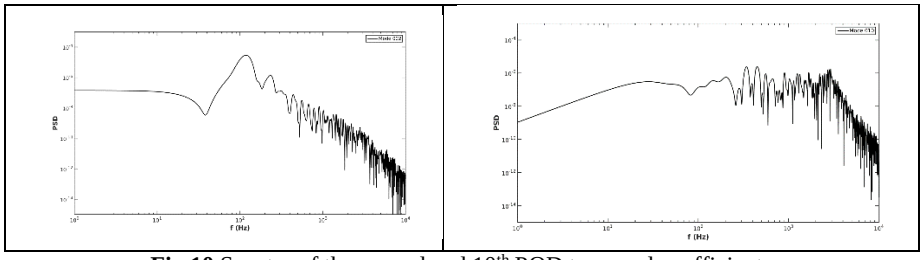

Fig.10 Spectra of the second and 10th POD temporal coefficients

3.2 The swept V2C wing

Figure 11 shows the instantaneous eddy-viscosity 3D field past the wing (fully turbulent case), according to the OES-k-ε modelling. The eddy viscosity displays an organization according to spatial smaller-scale wavelengths due to the above formation of coherent structures. A weak unsteadiness has been maintained at higher time values but is was found that for the present grid and turbulence model, a practically steady state has been reached concerning the forces and near-wall parameters. The effect of the transition position fixed by numerical tripping at 55% and 30% of the chord has been studied at 5° of incidence, because of the TFAST's main goal to provide 'laminarity' in respect of drag reduction.

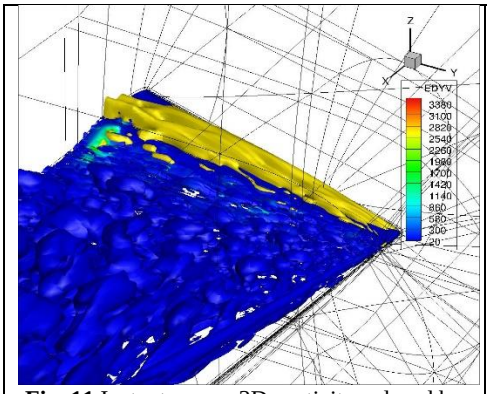

Fig. 11 Instantaneous 3D vorticity colored by iso-pressure contours, k-ω-OES, fully turbulent case, illustrating the undulation of the coherent vortex rows along the span, according to predominant wavelengths

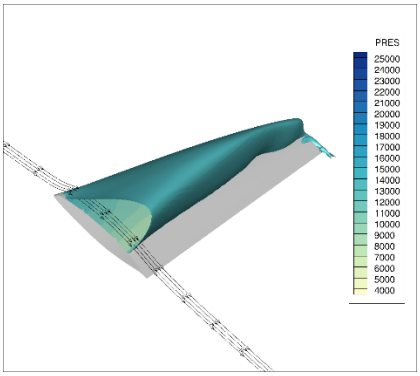

Fig. 17 Instantaneous iso-pressure surfaces along the span at t=0.1632 illustrating the shock formation along the span

Moreover, the choice of 5° is because for the present Mach number, this incidence is in the frontier of buffet onset. In case of a swept wing, the local Reynolds number based on the chord varies along the span. Therefore, only several

spanwise sections are over-critical regarding buffet. The interest of the present study is to depict the regions subjected to buffet onset.

Cases of 55% and 30% of fixed transition at 5° of incidence

Concerning the 55% case, Figure 12 shows the dimensional, non-normalised lift force versus time, displaying buffet oscillations among other smaller-scale fluctuations. This figure also shows the pressure coefficient at different spanwise positions, the value *y/c*=0.1 corresponding to the large chord spanwise sections side. It can be seen that towards the small chord side reaching *y/c*=0.9, the *Cp* evolution in the shock area progressively displays an inclination indicating buffet formation, as also shown on the lift coefficient oscillations. Figure 13 shows the iso-Mach contours for the 55% transition case for a mid-span section and for the *y/s*=0.9 one. A more detailed investigation of the buffet existence is necessary by using a finer grid, in order to provide a more detailed discussion.

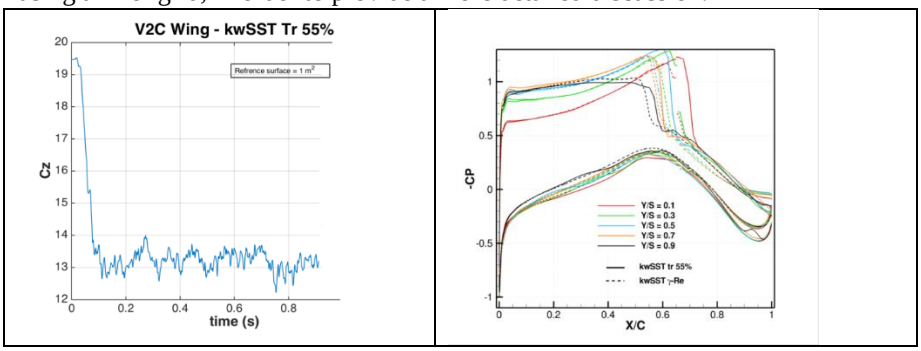

Fig.12 Left: time-dependent drag coefficient (not normalized by the reference surface)

Concerning the case of 30% fixed transition at 5° of incidence, this reached steady state, with mean drag coefficient 0.0423 and mean lift 0.796. The corresponding *Cp* coefficients at different spanwise positions is shown on Figure 14, where only normal shocks appear as expected in case of no buffet spatial amplitude. An onset of weak unsteadiness has been obtained in the near wake.

The case of 7° and fixed transition at 30% has been finally studied. Figure 15 shows pressure oscillations versus time indicating formation of buffet mode.

Case of 30% of fixed transition and 7° of incidence

This case displays an onset of buffet at a section located near the ¾ of the span towards the small chord free edge, as indicated by the pressure versus time at the wall point P4 shown in Figure 15. The iso-pressure contours of Figure 16 within a period show the shock motion, the thickening of the boundary layer, separation and formation of the von Kármán vortex street, all these being characteristics of buffet onset. Figure 17 shows the shock location along the span at t=0.1632s.

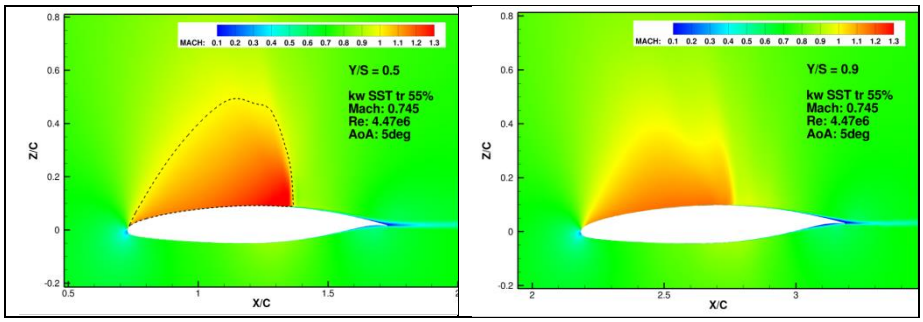

Fig.13 Iso-Mach contours at two spanwise positions. y/s=0.9 is located towards the small chord sections

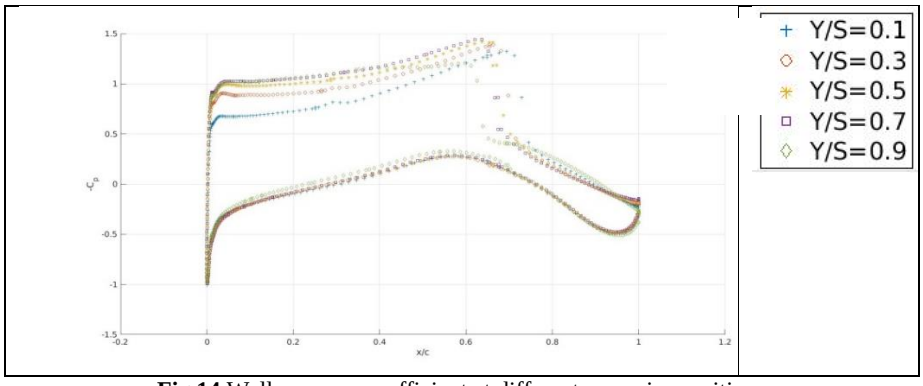

Fig.14 Wall pressure coefficient at different spanwise positions

4 Conclusion

A numerical study by means of statistical and hybrid turbulence modelling has been carried out to analyse the buffet phenomenon around a transonic wing of constant section and a swept wing at high Reynolds number. The predictions have shown the ability of all the methods in capturing the buffet's frequency bump, but at different spectral amplitudes and width of the bump. The DDES-SST simulations indicated a too strong suction effect and enhancement of the separation and of the shock's amplitude.

The OES simulations provided a moderate shock amplitude and a good comparison of the mean forces coefficients with the experiments carried out by the Institute of Aviation (Warsaw). A detailed POD study using the DDES-SST simulations shows the role of the most energetic modes in respect of the buffet spatial oscillation amplitude as well as the impact of higher-order modes in the shear layer dynamics.

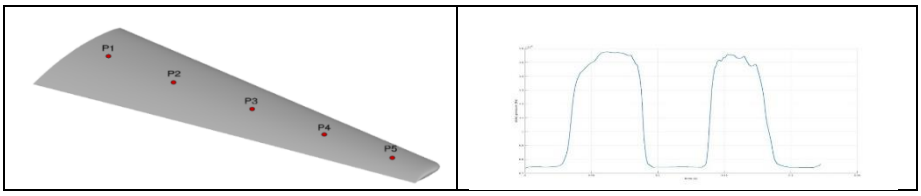

Fig.15 Constant section V2C wing: grid and zoom around the section

Concerning the swept wing, the fully turbulent case and the fixed transition at 30% of the chord lead to practically steady state at 5° of incidence by using the OES approach. The 55% of fixed transition displays a weak buffet towards the small chord dimensions. The case at 30% of transition and 7° of incidence displays buffet onset near the ¾ of the span, towards the smaller chord dimensions. These studies are continuing in the context of POD-based stochastic forcing enabling upscale turbulence modelling and towards a more detailed analysis of the buffet dynamics and modification along the span of the swept wing.

Acknowledgments This work has been part of the EU project TFAST, "Transition location effect on shock boundary layer interaction", coordinated by P. Doerffer - IMP-PAN - Gdansk, Poland and funded by the European Community represented by the CEC, Research Directorate-General, in the 7th Framework Programme, under Grant Agreement N° 265455. The authors are grateful for the use of the French supercomputing facilities of CINES, IDRIS, CALMIP which provided a significant CPU allocation. The authors thank the students of the BEI Bureau d'Etudes Approfondies of the Engineering school ENSEEIHT, Jean-Baptiste Tô, Julien Saint James and Julien Charcosset for their valuable contributions.

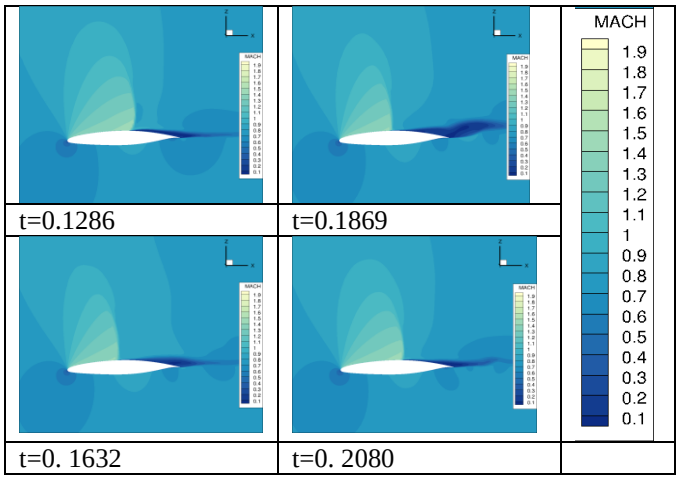

Fig. 16 Instantaneous iso-Cp at *y/s*=0.8 spanwise section showing formation of the buffet motion, associated with the boundary layer thickness, separation and the von Kármán mode in the near wake

References

1 R. Bourguet, M. Braza, G. Harran, R. El Akoury (2008), J. Fluids and Structures, 24 (8), 1240-1251, 2008.

2. M. Braza, R. Perrin, Y. Hoarau (2006), Turbulence Properties in the cylinder wake at high Reynolds number", J. Fluids and Structures, 22, pp. 757–771.
3. Cleansky European project, Call 11 - GRA-02-019, Advanced, high aspect ratio transonic laminar wing for regional aircraft with load controll & alleviation devices (2013–2016).
4. S. Deck, Numerical computation of transonic buffet over a supercritical airfoil, AIAA J. 43 (7) (2005) 1556–1566
5. F. Grossi, M. Braza, Y. Hoarau, Prediction of Transonic Buffet by Delayed Detached-Eddy Simulation, AIAA J., 52, N°10, 2014, pp. 2300-2312.
6. L. Jacquin, P. Molton, S. Deck, B. Maury, D. Soulevant, An experimental study of shock oscillation over a transonic supercritical profile, in: 35th AIAA Fluid Dynamics Conference and Exhibit, Toronto, Ontario, Canada, 2005, AIAA 2005-4902.
7. L. Jacquin, P. Molton, S. Deck, B. Maury, D. Soulevant, Experimental study of shock oscillation over a transonic supercritical profile, AIAA J. 47 (9) (2009) 1985–1994.
8. B.H.K. Lee, Oscillatory shock motion caused by transonic shock boundary-layer interaction, AIAA J. 28 (5) (1990) 942–944.
9. J.B. McDevitt, L.L. Levy Jr., G.S. Deiwert, Transonic flow about a thick circular arc airfoil, AIAA J. 14 (5) (1976) 606–613.
10. Menter, F. R., AIAA Journal, Vol. 32, No. 8, August 1994, pp. 1598-1605.
11. P.L. Roe, Approximate Riemann solvers, parameter vectors, and difference schemes, J. Comput. Phys. 43 (2) (1981) 357–372.
12. H.L. Seegmiller, J.G. Marvin, L.L. Levy Jr., Steady and unsteady transonic flow, AIAA J. 16 (12) (1978) 1262–1270.

13. P.R. Spalart, C.L. Rumsey, Effective inflow conditions for turbulence models in aerodynamic calculations, AIAA J. 45 (10) (2007) 2544–2553.
14. P.R. Spalart, S. Deck, M.L. Shur, K.D. Squires, M.K. Strelets, A. Travin, A new version of detached-eddy simulation, resistant to ambiguous grid densities, Theor. Comput. Fluid Dyn. 20 (6) (2006) 181–195.
15. D. Szubert, F. Grossi, A. Jimenez-Garcia, Y. Hoarau, J. Hunt, M. Braza, Shock-vortex shear-layer interaction in the transonic flow around a supercritical airfoil at high Reynolds number in buffet conditions, J. Fluids & Structures, 55, pp. 276–302, (2015).
16. D. Szubert, I. Asproulias, F. Grossi, R. Duvigneau, Y. Hoarau, M. Braza, Numerical study of the turbulent transonic interaction and transition location effect involving optimisation around a supercritical airfoil", European Journal of Mechanics-B/Fluids, 2015, 55, N° 2, pp. 380-393.
17. B. Van Leer, Towards the ultimate conservative difference scheme. V. A second order sequel to Godunov's method, J. Comput. Phys. 32 (1) (1979) 101–136.
18.. Vos J., Chaput E., Arlinger B., Rizzi A., and Corjon A., Recent advances in aerodynamics inside the NSMB (Navier-Stokes Multi-Block) consortium, AIAA Paper 1998-0802 (1998), Reno, USA.
19. Y. Hoarau, D. Pena, J. B. Vos, D. Charbonnier, A. Gehri, M. Braza, T. Deloze and E. Laurendeau, Recents Developments of the Navier-Stokes Multi-Block (NSMB) CFD solver, AIAA Paper 2016-2056 (2016), San Diego, USA.